Journal of Ultrafine Grained and Nanostructured Materials
https://jufgnsm.ut.ac.ir
Vol. 52, No.1, June 2019, pp. 110-121
Print ISSN: 2423-6845 Online ISSN: 2423-6837
DOI: 10.22059/JUFGNSM.2019.01.12

A Novel Approach for Direct Preparation of Hydroxyapatite Nanoparticles from Dog Bones using Microwave

Gholam Reza Khayati*, Farkhonde Ghanbari Rad

Department of Materials Science and Engineering, Shahid Bahonar University of Kerman, Kerman, Iran.

Recieved: 10 August 2018; Accepted: 27 September 2018

** Corresponding author email: khayati@uk.ac.ir*

ABSTRACT

Hydroxyapatite (HA) is one of the most common biocompatible ceramic with wide usages in various aspects of medicine due to the resemblance to the mineral bone tissue. The particle size of HA has a key roll in determination of the reaction rate at the interface of natural bones/artificial. Accordingly, this paper tries to propose a novel approach for the preparation of HA nanoparticles from natural source as raw materials using microwave irradiation without any further heat treatment. To compare the proposed approach various combination of micro irradiation and heat treatment as traditional and more recent developments were performed. Characterizations of products were carried out using XRD, SEM and TEM techniques. The results confirmed the presence of minor constituents (Mg, Sr, C, O) and the ratio of Ca/Mg=1.63 in the products. Moreover, the formation of relatively spherical shape like nanoparticles of hydroxyapatite (about 30 nm) was confirmed by TEM images during the direct preparation of HA nanoparticles by employment of microwave irradiation. According to the results, the proposed approach provide the possibility of the preparation of large-scale, spherical and pure HA nanoparticles in acceptable time by usage of low cost natural source, eco-friendly method without the using of organic solvent and expensive raw materials.

Keywords: *Microwave; Hydroxyapatite Nanoparticles; Natural bones; Heat treatment.*

1. Introduction

Hydroxyapatite (HA) is one of the most common bio-ceramic with wide applications in biomedical usages. There are various preparation routes in the literatures for the preparation of HA as precipitation approach [1], ultrasonic irradiation [2], sol-gel [3], electrodeposition [4], hydrothermal process [5] and spray pyrolysis [6]. Some of researches were carried out based on the using of natural sources, e.g., sea corals [7], egg shells [8], bovine bone [9], planet sources [10], fish bones and fish scales [11] as raw materials. The outstanding advantages of mammalian bones as raw materials are low cost, high purity and the presence of minor affecting elements such as Mg, Zr and Sr [9].

Todays, the advancement of microwave (MW) irradiation is a hot issue for preparation of biomaterials. In MW irradiation, internally generated heat of molecules is replaced by the external heating source and consequently more attractive due to the rapid heating, shorter process times, higher efficiently for every transformation as well as throughout volume heating. MW irradiation of eggshell to prepare the precursors in sol-gel technique [12, 13] and activation of aqueous solution for precipitation of Ca and P components using a domestics MW [14] were the typically usages of MW for HA preparation. Side by side

comparison of various techniques for preparation of HA are summerized in Table 1. Accordingly, the possibility of HA nanoparticles preparation by combination of MW irradiation and heat treatment

Table 1- Side by side comparison of various techniques for preparation of HA

No	Method	Main idea	Source	HA Grain size	Secondary phases	Morphology of products	Ref.
1	Heat treatment and chemical exchange reaction	Studding of the effect of excess diammonium phosphate on the formation of HA	Corals	–	β - $Ca_3(PO_4)_2$	Hexagonal	1996 [16]
2	Heat treatment	Proposing of possible route for producing of novel porous ceramics	Fish bone	200-500nm	$Ca_3(PO_4)_2$	Spherical	2002 [17]
3	Heat treatment and ball milling	Employment of Eggshells as raw materials by addition of P precursor	Eggshells	-	β - $Ca_3(PO_4)_2$ CaO	Grape-type granular	2003 [18]
4	Hydrothermal and microwave irradiation	Comparative crystallographic analysis of HA derived from the chemical route, coral and xenogeneic bone	Coral	-	-	Hexagonal	2004 [19]
5	Chemical process and heat treatment	Comparative crystallographic analysis of HA derived from the chemical route, coral and xenogeneic bone	Bovine bone	-	-	Hexagonal	2004 [19]
6	Hydrothermal and solvothermal	Employment of Coral shells as raw materials	Coral shells	-	$(Ca,Sr,Pb,Zn)CO_3$, $Ca_3(PO_4)_2$	Porous structure	2005 [20]
7	Microwave processing	Using of microwave For activation of eggshells as precursor	Eggshells	18nm	CaO	Spherulite	2007 [21]
8	Vibrio-milling	Employment of vibro-milling method	Bovine bone	58-62nm	–	Needle like	2008 [22]
9	Burning of bones and heat treatment	Heat treatment in two stages; Preparation of HA between at 950°C	Bovine bone	1-30μm	–	Irregular shape with wide size of distribution	2009 [23]
10	Thermal decomposition, subcritical water and alkaline hydrothermal processes	Production of small nanorod	Bovine bone	300nm	–	Nanorod	2009 [24]
11	Subcritical water and alkaline hydrothermal processes	Production of small nanoflakes	Bovine bone	>300nm	-	Nanoflakes	2009 [24]
12	Alkaline hydrothermal processes	Using of NaOH as dopant	Bovine bone	>300nm	-	Nanoflakes	2009 [24]

Table 1- Continued

13	Burning of bones; milling and heat treatment	Preparation of stable HA between 800 and 1100°C	Bovine bone	133nm	–	Irregular spheres	2009 [25]
14	Sol–gel method	Using of small quantities of biomolecules as additive to induce novel properties	Eggshells	50nm	-	Rectangular	2009 [26]
15	Sol–gel method	Decreasing of calcination temperature to 700°C respect to the literature	Eggshells	35-50nm	-	Prolate spheroidal	2009 [27]
16	Hydrothermal on the saturated vapor pressure curve	Analyses of crystallographic relationships during the hydrothermal conversion of a calcitic sea urchin spine into apatite	Sea urchin spines	-	-	Rod like	2010 [28]
17	Burning of bones and heat treatment	Evaluation of the effects of temperature on the microstructure of the calcined samples regarding porosity and pore size distribution.	Human, bovine and porcine	44-105nm	-	Porous structure	2010 [29]
18	Solvothermal method	Investigation of practical parameters on the adsorption of Pb	Eggshells	-	-	-	2010 [30]
19	Heat treatment of activated precursor after ball milling	Preparation technique	Oyster shells	-	β - $Ca_3(PO_4)_2$	Rod like	2011 [31]
20	Autoclaves and hydrothermal	Higher metabolically activity of low-crystalline apatite structures	Eggshells and fruits	12-49nm	-	Needle and rod like	2011 [32]
21	Transferred arc plasma (TAP)	Investigation of the effect of processing time on the preparation of organic free HA	Bovine bone	–	$Ca_3(PO_4)_2$; CaO	–	2011 [33]
22	Heat treatment	Preparation of HA containing silver nanoparticles	Bovine bone	8-20nm	-	Spherical and Hexagonal	2011 [34]
23	Heat treatment	Employment of fish bones as raw materials	Tuna and Sword bones	50-83nm	β - $Ca_3(PO_4)_2$	Rod like	2011 [35]
24	Burning of bones and heat treatment	Effects of calcination time and temperature	Bovine bone	–	$Ca_3(PO_4)_2$ and β - $Ca_3(PO_4)_2$	Hexagonal	2012 [36]
25	Precipitation method	Employment of eggshells as precursor in precipitation method	Eggshells	-	-	-	2012 [37]
26	Microwave; sol–gel	Employment of microwave for activation of precursor	Eggshells	78nm	β - $Ca_3(PO_4)_2$	Flower like	2012 [38]
27	Hydrothermal	Synthesis of HA by a simple hydrothermal method	Eggshells	0.06 μm	$CaHPO_4$	Whiskers	2012 [39]
28	Solvothermal method	Preparation of flower like at 120°C in appropriate time	Eggshells	35-15 μm	-	Flower like	2012 [40]
29	Precipitation technique	Investigation of pH and temperature in particle size of HA	Eggshells	35nm	$Ca_3(PO_4)_2$, $Ca_9(Mg,Fe^{2+})(PO_4)_6(PO_3OH)$	Like globules	2013 [41]

Table 1- Continued

30	Heat treatment	Treating the bones in solution before the annealing	Cod fish bones	300-500nm	β - $Ca_3(PO_4)_2$	Needle like	2013 [42]
31	Combination of thermal mechonochemical method	Investigation of the effects of milling and composition of raw materials on mechanochemical synthesis of HA	Bovine bone	116nm	–	Spheroidal and polygonal	2013 [43]
32	Heat treatment	Prediction of HA morphology by XRD	Bovine bone	29.5-79.1nm	-	Equiaxial with uniform porosity	2013 [44]
33	Heat treatment	Prediction of HA morphology by XRD	Bovine bone	73.1nm	-	Hexagonal	2013 [44]
34	Pyrolysis–wet slurry precipitation process	Synthesis method	Mussel shells	-	-	-	2013 [45]
35	Self-assisted chemical reaction method	Analysis of the effect of soaked in K_2HPO_4 solution for different days	Eggshells	41nm	-	Circular	2013 [46]
36	Solid state reaction	Using of $CaHPO_4$ $2H_2O$ and $Ca_2P_2O_7$ as precursors	Eggshells	-	β - $Ca_3(PO_4)_2$	Spheroidal	2013 [47]
37	Heat treatment	Comparison of synthetic and biological Hydroxyapatite	Bovine bone	-	-	Porous and Interconnected	2013 [48]
37	Alkaline treatment	Using of NaOH as dopant	Bovine bone	-	-	Some pores but is still dense	2013 [48]
37	Defat (Treatment to remove fat)	Using of Petroleum ether acetone as dopant	Bovine bone	-	-	Dense surface	2013 [48]
38	Heat treatment	In vitro bioactivity and in vitro degradation behaviors of the composites prepared by HA	Bovine bone	20nm	-	Spherical	2014 [49]
39	Pyrolysis process followed by a chemical synthesis step at ambient pressure and temperature of 100°C under alkaline condition	Production of HA with porous structure	Shells	-	$CaCO_3$ $Ca_3(PO_4)_2$	Porous and interconnected structure	2015 [50]
40	Heat treatment	Studding the mechanism of HA nucleation	Cattle bone	37.15nm	-	Needle shape	2015 [51]
41	Precipitation method and microwave activation	Production of nanocomposite films by green synthesis	Eggshells	4 -14 nm	–	Needle-like	2015 [52]

Table 1- Continued

42	Chemicals and microwave irradiation	Using ethylenediaminetetra acetic acid as chelating agent through microwave irradiation	Mussel shell	Length 100–200 nm and width 2–5 nm	-	Flower-like	2016 [53]
43	Heat treatment	Using of fish bone as raw materials	Fish bone	64-330nm	–	–	2016 [54]
44	Alkaline treatment	Preparation of HA from fish scale wastes for selenium adsorption	Tilapia nilotica scales	10-25nm	-	Hexagonal	2017 [55]
45	Enzymatic hydrolysis	Extraction of HA from fish scale using enzymatic hydrolysis	Oreochromis sp. scales	719.8nm	-	Irregular spherical	2017 [56]
46	Alkaline hydrolysis	Employment of Thunnus obesus bone as raw material	Thunnus obesus bone	Length 17–71 nm and width 5–10 nm	-	Rod like	2017 [57]
47	Heat treatment	Characterization of optical properties of natural HA, investigation of calcination time and milling time	Pseudoplatystoma corruscans, Paulicea lutkeni, Pseudoplatystoma fasciatum bones	300nm	-	-	2017 [58]
48	Heat treatment	Investigation of the kinetics and mechanism of transformation	Sepia officinalis bones	200-300nm	$CaHPO.2H_2O$	Rod	2017 [59]

of naturally source, especially dog bones with nearly the same of human bones biological behavior [15], hasn't investigated, yet. The present study proposed a new method on the base of MW irradiation and heat treatment of dog bones as raw materials for the preparation of HA nanoparticles.

2. Experimental details

Dog bones were collected and removed all skeletal flesh from there's. Clean bones dropped at boiled water for 60 min and dried for 24 h at room temperature. The dried bones were manually scraped and sieved to prepare a mesh size lower than 4 mm and hold to -19 °C for 30 min.

Bones particles divided to 5 samples, each sample experiences various heating treatment and MW irradiation as shown in Table 2. MW Irradiation was done in silicon carbide vessel. Phase characterizations of products carried out by Philips PW- 1730 X-ray diffraction (XRD) using Cu K_{α} radiation. The average crystallite size was estimated using Scherrer's equation [60-62]. The morphology, point chemical analysis and size distribution of samples investigated by SEM (JEOLJSM 5310), dispersive energy X-Ray spectroscopy (EDX) (Oxford Instrument) and TEM (CM200 Philips), respectively. To draw the histogram of size distribution, the average size of 85 particles in TEM images were measured using the microstructure measurement program.

3. Results and discussion

3.1. Changes in samples colors

As shown in Fig. 1, the color of raw bone (S1 sample) is pale yellow. After the heating of S2 sample at 600 °C for 150 min, its color changes to black. While, the same heating process after 10 min MW irradiation causes to the change in color to white (S3 sample). Moreover, MW irradiation for 30 min without any further heating is able to create similar color change in S5 sample. Also, by increasing the temperature from 600 °C (in S3 sample) to 900 °C (in S4 sample) the color of sample remained relatively constant.

Generally, the mammalian bones consist of hydroxyapatite and carbon constituents distributed in the amorphous organized collagen fibers matrix. Removal of organic constituents, phase transformation of bones, changing the amount and degree of crystallity during the heat treatment and MW irradiation were the main reasons of the samples color changes in Fig. 1. Since, the raw samples holds in -19 °C before irradiation, it can be concluded that the thermal shock of initially samples induced the micro cracks/flaws in the structure and enhanced the internal surface of samples during the irradiation. In this case, the surface of flaws acts as suitable situation for the exitance of burning products and the evolution of crystalline HA.

It was necessary to note that, the main difference between MW energy and other forms of radiation, e.g., X and gamma rays, are the MW energy is non-ionizing and therefore does not change the molecular structure of the compounds during the heating [63]. Accordingly, MW irradiation provides only thermal activation. Due to the low dielectric constant of raw dog bones [64], it has low potential for the coupling with microwaves. According to the results, irradiation of dog bone in the substrate with little dielectric constant has not any effect on the evolution of HA. While, doing the same experiment on silicon carbide solid cup provide the required energy for the evolution of HA at 30 min irradiation time. As a consequence, the time and intensity of MW during the irradiation of raw dog bone directly enhanced the amount of prepared heat energy as well as the maximum of operational temperature. In this condition, the crystallity and grain size of HA must be enhanced, directly.

3.2. XRD phase identification

Bone composed from amorphous organized

Table 2- Various conditions for the preparation of samples

Sample	MW activation	Time of MW (min)	Calcination temperature (°C)	Calcination Time (min)
S1	✗	✗	✗	✗
S2	✗	✗	600	150
S3	✓	10	600	150
S4	✓	10	900	150
S5	✓	30	✗	✗

Fig. 1- The changes of dog bone colors during the heat treatment and MW irradiation for S1: Raw bone; S2: Raw bone after heating at 600 °C for 150 min; S3: Sample after 10 min MW irradiation and then heating at 600 °C for 150 min; S4: Sample after 10 min MW irradiation and then heating at 900 °C for 150 min; S5: Sample after 30 min MW irradiation.

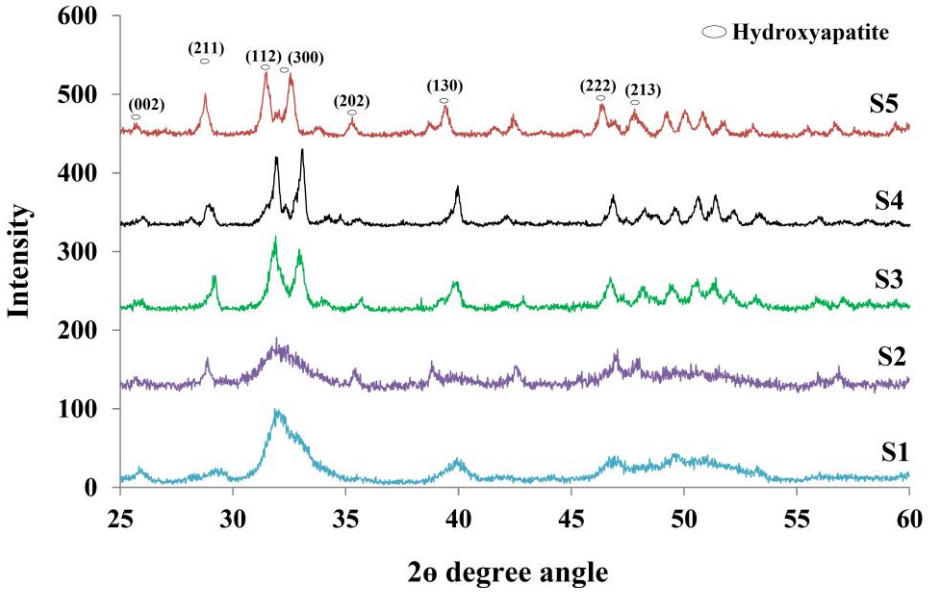

Fig. 2- XRD spectra of dog bones after various heating treatment and MW irradiation for S1: Raw bone; S2: Raw bone after heating at 600 °C for 150 min; S3: Sample after 10 min MW irradiation and then heating at 600 °C for 150 min; S4: Sample after 10 min MW irradiation and then heating at 900 °C for 150 min; S5: Sample after 30 min MW irradiation.

collagen fibers as a matrix, embedded with HA nanocrystals [65]. The XRD patterns of various samples (Fig. 2) confirmed the presence of HA (JCPDS cod nom: 01-072-1243). As shown all peaks are broader compared to the standard, especially in S1 and S2 samples, confirmed the presence of amorphous and crystalline combination phases of organized collagen and HA, respectively. All samples have sharp peaks of (002) diffractions due to the induction of the co-alignment between the c-axis of the HA crystals and the long axis of the matrix collagen [66]. Other peaks are merged at (300), (112) and (211) planes especially in S1 sample. Also, the number and intensity of characteristics peaks of S3, S4 and S5 samples are increased, respect to S1 and S2 samples. It is related to the formation and increasing the crystallinity of HA phase after MW irradiation and heat treatment. Similar to the changes in colors in Fig. 1; S3, S4 and S5 samples experience the same phases evolution. Consequently, MW irradiation of raw bone for 30 min in S5 sample is able to produce crystalline phase of HA, successfully.

Table 3 abbreviates the unit cell parameters of S3 and S4 samples. As shown the unit cell dimension are relatively constant at 600 °C and 900 °C after 150 min, and confirm the stable nature of HA nanoparticles.

Using Scherres equation, the average crystallite sizes of products are measured to be about 29±1 nm, 45±1 nm and 67±1 nm for S3, S4 and S5 samples, respectively. Thus, increasing the heating temperatures from 600 °C to 900 °C, improved the enlargement of grain boundaries and as a consequence, crystallite size enhanced by heating temperature. From macroscopic view, reducing of total surface energy is the driving force for the coarsening and microscopically, decreasing in surface energy with various curvatures was strongly improved mass transport in higher temperature [67]. Moreover, MW irradiation for higher time (30 min in sample S5) enable us to produce HA nanocrystalline similar to S3 and S4 samples. It was necessary to note that, the energy of MW in S5 sample is higher then the S3 and S4 samples, due to the higher crystallite size of S5 sample. Because of the lower crystallite size of HA within the crystalline samples and the novelty of preparation method, S3 and S5 samples were selected for further microstructure investigation by SEM and TEM techniques.

Fig. 3 represents the SEM images and typical point chemical analysis (EDX spectra) of S3 sample prepared at 600 °C. Accordingly, the product

Table 3- Unit cell parameters of HA powder for S3 and S4 samples

Sample	Unit cell parameter (Å)		Cell volume ($Å^3$)
	A	C	
S3	9.3	6.8	522.2
S4	9.3	6.8	522.8

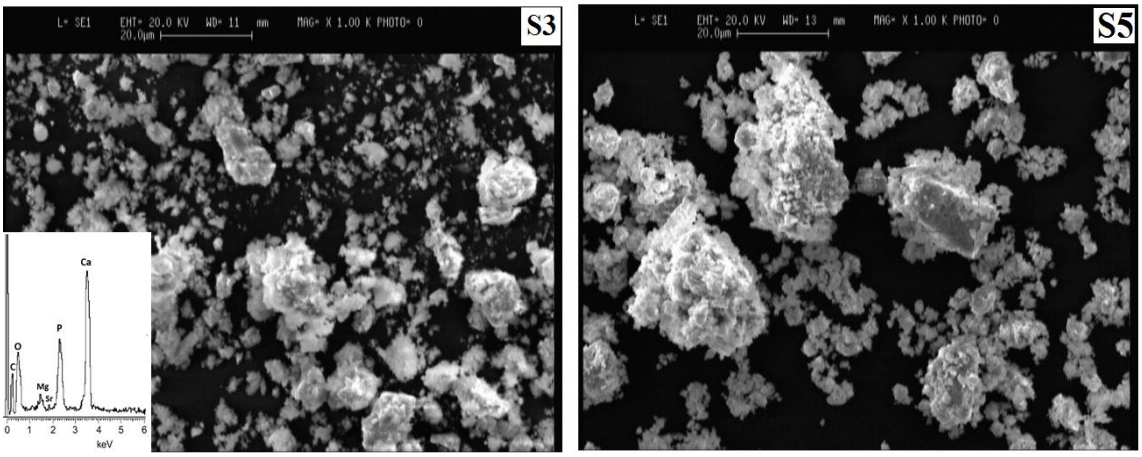

Fig. 3- SEM images of S3: Sample after 10 min MW irradiation and then heating at 600 °C for 150 min and S5: Sample after 30 min MW irradiation.

particles have generally rounded morphology with the strong tendency for sever agglomeration to compensate the surface effects. EDS spectra confirms the presence of minor affecting elements (e.g., Mg, O, Sr and C) in the products as well as the ratio of Ca/P= 1.63. This ratio is close to the stoichiometric ratio of Ca/P in HA (about 1.67). Since, Mg and Sr are categorized in vital constituents for tissue metabolic activities, their presence are so beneficially from biological aspects. By decreasing the ratio of Ca/P in HA, calcium deficient hydroxyapatite (CDHA) is produced. CDHA transforms to β-tricalcium phosphate (β -TCP) beyond 600 °C [68-70]. Since, there is not any peak/s that confirmed the formation of β -TCP up to 900 °C (in S4 sample), the precursor doesn't belong to CDHA family. As shown in Fig. 3 (S5 sample), the tendency for agglomeration was severer than the S3 sample. This can be related to the higher shape irregularity and size distribution of particles in S5 sample. This evident confirmed by TEM observations in Fig. 4. It was necessary to note that the EDX spectra and point chemical analysis of S5 is similar to S3 sample.

Fig. 4 shows the TEM images and their size distribution histogram of HA prepared at 600 °C for 150 min after 10 min MW irradiation (S3 sample) and HA prepared after 30 min MW irradiation (S5 sample). Similar to the XRD results, the average size of particles is to be about 30 nm (S3 sample in Fig. 4). While, the size distribution of S5 sample is higher and equal to be about 55 nm. Also, due to the severity of MW irradiation the average particles size of HA in S5 is higher than S3.

Since, the thermal activation is the main effect of MW during the irradiation, it can be concluded that by enhancement of the intensity and duration of MW irradiation from 10 min (S3 samples) to

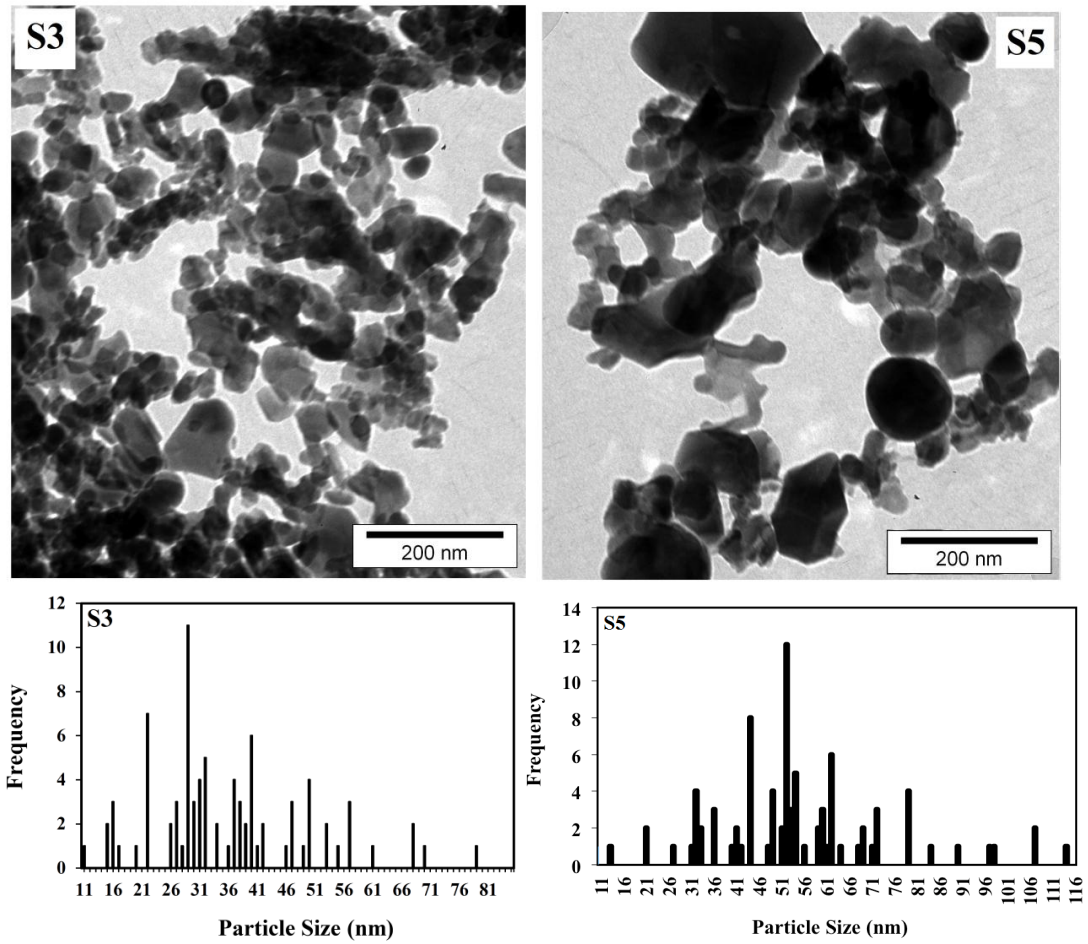

Fig. 4- TEM images of S3: Sample after 10 min MW irradiation and then heating at 600 °C for 150 min and S5: Sample after 30 min MW irradiation.

30 min (in S5 sample), the required energy for the burning of organic compound of raw bone, i.e., carbon constituent, amorphous organized collagen fibers matrix and the evolution of HA nanoparticles have been provided.

From morphological aspects, in the case of 30 min MW irradiation, the HA particles has more tendency for growth and preparation of spherical morphology with narrower distribution size. It was necessary to note that the coarsening tendency of grains that accelerates at high temperatures can be explained by Ostwald ripening and Oriented attachment mechanisms [71-72]. The former is administrated for more soluble materials and the dissolution of the smaller ones caused to the growth of the larger particles/crystals. While, the later is administrated for less soluble crystals and merging of the smaller ones each other caused to the coarsening of particles. More stability of larger particles/crystals than the smaller ones is the driving force of Ostwald ripening and is a function of temperature due to its effect on the interfacial energy, growth rate coefficients, and solubility. While, the decreasing of interphase boundary as well as the surface energy of the system are the driving force of Oriented attachment. Both mechanisms dependent to the amount of diffusion dictated by "kT" value and enhanced at higher temperatures. Since, the composition of HA is consistent in our experiments the Oriented attachment mechanism was more effective.

4. Conclusion

In this study, HA nanoparticles were successfully prepared by combination of MW irradiation and heat treatment of dog bones as precursor. The same nano-HA with higher particles size is produced after 30 min of MW irradiation in comparison of the sample prepared after 10 min MW irradiation and then heating at 600 °C for 150 min. It can be concluded that, by optimization of practical parameter of MW in the future, it will possible to prepare the nano-HA from dog bone with the highest similarity to the human bones from biological aspects. Since, the proposed method doesn't require to the high extensive purity precursor, complicated equipment as well as acceptable biocompatibility with the human bones, is superior to the other existed procedures for preparation of HA nanoparticles.

References

1. Santos MH, Oliveira MD, Souza LP, Mansur HS, Vasconcelos WL. Synthesis control and characterization of hydroxyapatite prepared by wet precipitation process. Materials Research. 2004 Dec;7(4):625-30.
2. Kojima Y, Kitazawa K, Nishimiya N. Synthesis of nano-sized hydroxyapatite by ultrasound irradiation. Journal of Physics: Conference Series. 2012;339:012001.
3. Masuda Y, Matubara K, Sakka S. Synthesis of Hydroxyapatite from Metal Alkoxides through Sot-Gel Technique. Journal of the Ceramic Society of Japan. 1990;98(1143):1255-66.
4. Shirkhanzadeh M. Journal of Materials Science Materials in Medicine. 1998;9(2):67-72.
5. Suchanek WL, Riman RE. Hydrothermal Synthesis of Advanced Ceramic Powders. Advances in Science and Technology. 2006;45:184-93.
6. Cho JS, Kang YC. Nano-sized hydroxyapatite powders prepared by flame spray pyrolysis. Journal of Alloys and Compounds. 2008;464(1-2):282-7.
7. Sivakumar M, Kumar TSS, Shantha KL, Rao KP. Development of hydroxyapatite derived from Indian coral. Biomaterials. 1996;17(17):1709-14.
8. Siva Rama Krishna D, Siddharthan A, Seshadri SK, Sampath Kumar TS. A novel route for synthesis of nanocrystalline hydroxyapatite from eggshell waste. Journal of Materials Science: Materials in Medicine. 2007;18(9):1735-43.
9. Murugan R, Ramakrishna S, Panduranga Rao K. Nanoporous hydroxy-carbonate apatite scaffold made of natural bone. Materials Letters. 2006;60(23):2844-7.
10. Tampieri A, Sprio S, Ruffini A, Celotti G, Lesci IG, Roveri N. From wood to bone: multi-step process to convert wood hierarchical structures into biomimetic hydroxyapatite scaffolds for bone tissue engineering. Journal of Materials Chemistry. 2009;19(28):4973.
11. Ozawa M, Suzuki S. Microstructural Development of Natural Hydroxyapatite Originated from Fish-Bone Waste through Heat Treatment. Journal of the American Ceramic Society. 2004;85(5):1315-7.
12. Hassan MN, Mahmoud MM, El-Fattah AA, Kandil S. Microwave-assisted preparation of Nano-hydroxyapatite for bone substitutes. Ceramics International. 2016;42(3):3725-44.
13. Kumar GS, Thamizhavel A, Girija EK. Microwave conversion of eggshells into flower-like hydroxyapatite nanostructure for biomedical applications. Materials Letters. 2012;76:198-200.
14. Lerner E, Sarig S, Azoury R. Enhanced maturation of hydroxyapatite from aqueous solutions using microwave irradiation. Journal of Materials Science: Materials in Medicine. 1991;2(3):138-41.
15. Aerssens J, Boonen S, Lowet G, Dequeker J. Interspecies Differences in Bone Composition, Density, and Quality: Potential Implications forin VivoBone Research1. Endocrinology. 1998;139(2):663-70.
16. Sivakumar M, Kumar TSS, Shantha KL, Rao KP. Development of hydroxyapatite derived from Indian coral. Biomaterials. 1996;17(17):1709-14.
17. Ozawa M, Suzuki S. Microstructural Development of Natural Hydroxyapatite Originated from Fish-Bone Waste through Heat Treatment. Journal of the American Ceramic Society. 2004;85(5):1315-7.
18. Lee SJ, Oh SH. Fabrication of calcium phosphate bioceramics by using eggshell and phosphoric acid. Materials Letters. 2003;57(29):4570-4.
19. Murugan R, Ramakrishna S. Crystallographic Study of Hydroxyapatite Bioceramics Derived from Various Sources. Crystal Growth & Design. 2005;5(1):111-2.
20. Kim YH, Song H, Riu DH, Kim SR, Kim HJ, Moon JH. Preparation of porous Si-incorporated hydroxyapatite. Current Applied Physics. 2005;5(5):538-41.
21. Siva Rama Krishna D, Siddharthan A, Seshadri SK, Sampath

Kumar TS. A novel route for synthesis of nanocrystalline hydroxyapatite from eggshell waste. Journal of Materials Science: Materials in Medicine. 2007;18(9):1735-43.
22. Ruksudjarit A, Pengpat K, Rujijanagul G, Tunkasiri T. Synthesis and characterization of nanocrystalline hydroxyapatite from natural bovine bone. Current Applied Physics. 2008;8(3-4):270-2.
23. Sobczak A, Kida A, Kowalski Z, Wzorek Z. Evaluation of the biomedical properties of hydroxyapatite obtained from bone waste. Polish Journal of Chemical Technology. 2009;11(1):37-43.
24. Barakat NAM, Khil MS, Omran AM, Sheikh FA, Kim HY. Extraction of pure natural hydroxyapatite from the bovine bones bio waste by three different methods. Journal of Materials Processing Technology. 2009;209(7):3408-15.
25. Javidi M, Javadpour S, Bahrololoom ME, Ma J. Electrophoretic Deposition of Natural Hydroxyapatite. Key Engineering Materials. 2009;412:183-8.
26. Nayar S, Guha A. Waste utilization for the controlled synthesis of nanosized hydroxyapatite. Materials Science and Engineering: C. 2009;29(4):1326-9.
27. Sanosh KP, Chu M-C, Balakrishnan A, Kim TN, Cho S-J. Utilization of biowaste eggshells to synthesize nanocrystalline hydroxyapatite powders. Materials Letters. 2009;63(24-25):2100-2.
28. Álvarez-Lloret P, Rodríguez-Navarro AB, Falini G, Fermani S, Ortega-Huertas M. Crystallographic Control of the Hydrothermal Conversion of Calcitic Sea Urchin Spine (Paracentrotus lividus) into Apatite. Crystal Growth & Design. 2010;10(12):5227-32.
29. Figueiredo M, Fernando A, Martins G, Freitas J, Judas F, Figueiredo H. Effect of the calcination temperature on the composition and microstructure of hydroxyapatite derived from human and animal bone. Ceramics International. 2010;36(8):2383-93.
30. Meski S, Ziani S, Khireddine H. Removal of Lead Ions by Hydroxyapatite Prepared from the Egg Shell. Journal of Chemical & Engineering Data. 2010;55(9):3923-8.
31. Wu S-C, Hsu H-C, Wu Y-N, Ho W-F. Hydroxyapatite synthesized from oyster shell powders by ball milling and heat treatment. Materials Characterization. 2011;62(12):1180-7.
32. Wu S-C, Tsou H-K, Hsu H-C, Hsu S-K, Liou S-P, Ho W-F. A hydrothermal synthesis of eggshell and fruit waste extract to produce nanosized hydroxyapatite. Ceramics International. 2013;39(7):8183-8.
33. Yoganand CP, Selvarajan V, Goudouri OM, Paraskevopoulos KM, Wu J, Xue D. Preparation of bovine hydroxyapatite by transferred arc plasma. Current Applied Physics. 2011;11(3):702-9.
34. Nirmala R, Sheikh FA, Kanjwal MA, Lee JH, Park S-J, Navamathavan R, et al. Synthesis and characterization of bovine femur bone hydroxyapatite containing silver nanoparticles for the biomedical applications. Journal of Nanoparticle Research. 2010;13(5):1917-27.
35. Boutinguiza M, Pou J, Comesaña R, Lusquiños F, de Carlos A, León B. Biological hydroxyapatite obtained from fish bones. Materials Science and Engineering: C. 2012;32(3):478-86.
36. Kusrini E, Sontang M. Characterization of x-ray diffraction and electron spin resonance: Effects of sintering time and temperature on bovine hydroxyapatite. Radiation Physics and Chemistry. 2012;81(2):118-25.
37. Habib F, Alam S, Zahra N, Irfan M, Iqbal W. Synthesis route and characterization of hydroxyapatite powder prepared from waste egg shells. Journal of the Chemical Society of Pakistan. 2012 30;34(3).
38. Kumar GS, Thamizhavel A, Girija EK. Microwave conversion of eggshells into flower-like hydroxyapatite nanostructure for biomedical applications. Materials Letters. 2012;76:198-200.
39. Elizondo-Villarreal N, Martínez-de-la-Cruz A, Guerra RO, Gómez-Ortega JL, Torres-Martínez LM, Castaño VM. Biomaterials from Agricultural Waste: Eggshell-based Hydroxyapatite. Water, Air, & Soil Pollution. 2012;223(7):3643-6.
40. Li S, Wang J, Jing X, Liu Q, Saba J, Mann T, et al. Conversion of Calcined Eggshells into Flower-Like Hydroxyapatite Agglomerates by Solvothermal Method Using Hydrogen Peroxide/N,N-Dimethylformamide Mixed Solvents. Journal of the American Ceramic Society. 2012;95(11):3377-9.
41. Goloshchapov DL, Kashkarov VM, Rumyantseva NA, Seredin PV, Lenshin AS, Agapov BL, et al. Synthesis of nanocrystalline hydroxyapatite by precipitation using hen's eggshell. Ceramics International. 2013;39(4):4539-49.
42. Piccirillo C, Silva MF, Pullar RC, Braga da Cruz I, Jorge R, Pintado MME, et al. Extraction and characterisation of apatite- and tricalcium phosphate-based materials from cod fish bones. Materials Science and Engineering: C. 2013;33(1):103-10.
43. Nasiri-Tabrizi B, Fahami A, Ebrahimi-Kahrizsangi R. A comparative study of hydroxyapatite nanostructures produced under different milling conditions and thermal treatment of bovine bone. Journal of Industrial and Engineering Chemistry. 2014;20(1):245-58.
44. Pramanik S, Hanif A, Pingguan-Murphy B, Abu Osman N. Morphological Change of Heat Treated Bovine Bone: A Comparative Study. Materials. 2012;6(1):65-75.
45. Shariffuddin JH, Jones MI, Patterson DA. Greener photocatalysts: Hydroxyapatite derived from waste mussel shells for the photocatalytic degradation of a model azo dye wastewater. Chemical Engineering Research and Design. 2013;91(9):1693-704.
46. Chaudhuri B, Mondal B, Modak DK, Pramanik K, Chaudhuri BK. Preparation and characterization of nanocrystalline hydroxyapatite from egg shell and K2HPO4 solution. Materials Letters. 2013;97:148-50.
47. Ho W-F, Hsu H-C, Hsu S-K, Hung C-W, Wu S-C. Calcium phosphate bioceramics synthesized from eggshell powders through a solid state reaction. Ceramics International. 2013;39(6):6467-73.
48. Giraldo-Betancur AL, Espinosa-Arbelaez DG, Real-López Ad, Millan-Malo BM, Rivera-Muñoz EM, Gutierrez-Cortez E, et al. Comparison of physicochemical properties of bio and commercial hydroxyapatite. Current Applied Physics. 2013;13(7):1383-90.
49. Rakmae S, Lorprayoon C, Ekgasit S, Suppakarn N. Influence of Heat-Treated Bovine Bone-Derived Hydroxyapatite on Physical Properties andin vitroDegradation Behavior of Poly (Lactic Acid) Composites. Polymer-Plastics Technology and Engineering. 2013;52(10):1043-53.
50. Shavandi A, Wilton V, Bekhit AE-DA. Synthesis of macro and micro porous hydroxyapatite (HA) structure from waste kina (Evechinus chloroticus) shells. Journal of the Taiwan Institute of Chemical Engineers. 2016;65:437-43.
51. Patel S, Wei S, Han J, Gao W. Transmission electron microscopy analysis of hydroxyapatite nanocrystals from cattle bones. Materials Characterization. 2015;109:73-8.
52. Rahman MM, Netravali AN, Tiimob BJ, Apalangya V, Rangari VK. Bio-inspired "green" nanocomposite using hydroxyapatite synthesized from eggshell waste and soy protein. Journal of Applied Polymer Science. 2016;133(22):n/a-n/a.
53. Kumar GS, Girija EK, Venkatesh M, Karunakaran G, Kolesnikov E, Kuznetsov D. One step method to synthesize flower-like hydroxyapatite architecture using mussel shell bio-waste as a calcium source. Ceramics International. 2017;43(3):3457-61.
54. Sunil BR, Jagannatham M. Producing hydroxyapatite from fish bones by heat treatment. Materials Letters. 2016;185:411-4.
55. Kongsri S, Janpradit K, Buapa K, Techawongstien S, Chanthai S. Nanocrystalline hydroxyapatite from fish scale waste: Preparation, characterization and application for selenium adsorption in aqueous solution. Chemical Engineering Journal. 2013;215-216:522-32.
56. Huang Y-C, Hsiao P-C, Chai H-J. Hydroxyapatite extracted from fish scale: Effects on MG63 osteoblast-like cells. Ceramics International. 2011;37(6):1825-31.
57. Venkatesan J, Qian ZJ, Ryu B, Thomas NV, Kim SK. A

comparative study of thermal calcination and an alkaline hydrolysis method in the isolation of hydroxyapatite fromThunnus obesusbone. Biomedical Materials. 2011;6(3):035003.
58. Coelho TM, Nogueira ES, Steimacher A, Medina AN, Weinand WR, Lima WM, et al. Characterization of natural nanostructured hydroxyapatite obtained from the bones of Brazilian river fish. Journal of Applied Physics. 2006;100(9):094312.
59. Ivankovic H, Tkalcec E, Orlic S, Gallego Ferrer G, Schauperl Z. Hydroxyapatite formation from cuttlefish bones: kinetics. Journal of Materials Science: Materials in Medicine. 2010;21(10):2711-22.
60. Katchova AL. Peter J. Barry and Paul N. Ellinger. Financial Management in Agriculture (7th ed.).Upper Saddle River, NJ: Prentice Hall, 2012, 408 pp., ISBN 9780135037591. $97. Agribusiness. 2012;28(2):239-40.
61. Howie RA. (H.) Lipson and (H.) Steeple Interpretation of X-ray powder diffraction patterns. London (Macmillan) and New York (St. Martins Press), 1970. Mineralogical Magazine. 1972;38(299):907.
62. Reza Khayati G, Dalvand H, Darezereshki E, Irannejad A. A facile method to synthesis of CdO nanoparticles from spent Ni–Cd batteries. Materials Letters. 2014;115:272-4.
63. Sanghi R. Microwave irradiation. Resonance. 2000;5(3):77-81.
64. Bowen CR, Gittings J, Turner IG, Baxter F, Chaudhuri JB. Dielectric and piezoelectric properties of hydroxyapatite-BaTiO3 composites. Applied Physics Letters. 2006;89(13):132906.
65. Posner AS. Crystal chemistry of bone mineral. Physiological Reviews. 1969;49(4):760-92.
66. Wang Y, Azaïs T, Robin M, Vallée A, Catania C, Legriel P, et al. The predominant role of collagen in the nucleation, growth, structure and orientation of bone apatite. Nature Materials. 2012;11(8):724-33.
67. Khayati GR, Janghorban K. An investigation on the application of process control agents in the preparation and consolidation behavior of nanocrystalline silver by mechanochemical method. Advanced Powder Technology. 2012;23(6):808-13.
68. Siddharthan A, Seshadri SK, Kumar TSS. Microwave accelerated synthesis of nanosized calcium deficient hydroxyapatite. Journal of Materials Science: Materials in Medicine. 2004;15(12):1279-84.
69. Siddharthan A, Sampath Kumar TS, Seshadri SK. Synthesis and characterization of nanocrystalline apatites from eggshells at different Ca/P ratios. Biomedical Materials. 2009;4(4):045010.
70. Siddharthan A, Seshadri SK, Kumar TS. Rapid synthesis of calcium deficient hydroxyapatite nanoparticles by microwave irradiation. Trends Biomater Artif Organs. 2005;18(2):110-3.
71. Xue X, Penn RL, Leite ER, Huang F, Lin Z. Crystal growth by oriented attachment: kinetic models and control factors. CrystEngComm. 2014;16(8):1419.
72. Madras G, McCoy BJ. Temperature effects during Ostwald ripening. The Journal of Chemical Physics. 2003;119(3):1683-93.